Hindawi
Geofluids
Volume 2021, Article ID 5579169, 14 pages
https://doi.org/10.1155/2021/5579169

Research Article

Three-Dimensional Morphology and Connectivity of Organic Pores in Shale from the Wufeng and Longmaxi Formations at the Southeast Sichuan Basin in China

Tao Jiang,[1,2,3,4] **Zhijun Jin**,[1,2,3,5] **Zongquan Hu**,[1,2,3] **Wei Du**,[1,2,3] **Zhongbao Liu**,[1,2,3] **and Jianhua Zhao**[1,2,3,6]

[1]*State Key Laboratory of Shale Oil and Gas Enrichment Mechanisms and Effective Development, Beijing 100083, China*
[2]*Key Laboratory of Shale Oil/Gas Exploration and Production, SINOPEC, Beijing 100083, China*
[3]*Petroleum Exploration and Production Research Institute, SINOPEC, Beijing 100083, China*
[4]*SinoProbe Center, Chinese Academy of Geological Sciences and China Geological Survey, Beijing 100037, China*
[5]*Institute of Energy, Peking University, Beijing 100871, China*
[6]*School of Geosciences, China University of Petroleum (East China), Qingdao 266580, China*

Correspondence should be addressed to Tao Jiang; jiangt813@cags.ac.cn

Received 22 January 2021; Accepted 22 April 2021; Published 17 May 2021

Academic Editor: Kun Zhang

Organic pores play an important role in shale reservoirs. Organic pores occur where shale gas was produced and accumulated. However, there is little scientific understanding of the distribution and connectivity of organic pores. Organic pore types and their structural characteristics were studied using a total organic carbon (TOC), thin section, focused ion beam scanning electron microscope (FIB-SEM), and nano-CT. The samples were from the Wufeng Formation in the Upper Ordovician and Longmaxi Formations from the lower Silurian. The results show that organic matter is mainly concentrated in the Wufeng Formation and the bottom of the Longmaxi Formation and that the middle and upper parts of the Longmaxi Formation contain a low amount of organic matter. The shale of the Wufeng-Longmaxi Formation has high maturity, and its organic pores are well developed. There are three types of organic pores: algae, graptolite, and pyrobitumen pores. The pore connectivity of shale with a high organic content is better than that of shale with a low organic content. The volume of the organic pores accounts for more than 50% of the volume of the organic matter. Majority of the organic pores have an aperture smaller than 100 nm and are round, nearly circular, and elliptical in morphology. Most of the organic pores in a shale formation are developed in pyrobitumen, and most of the larger organic pores are concentrated at the center of solid pyrobitumen. The organic pores in pyrobitumen have the best connectivity and are the most favorable reservoir spaces and migration channels for shale gas, which is a crucial point of reference for future research of shale gas.

1. Introduction

In recent years, shale gas has undergone significant development as an unconventional resource [1]. With the success of industrial shale gas development in the United States, the research and development of shale gas have become important for increasing global oil and gas resources [2]. With rising energy demand, increasing pressure on energy, and growing environmental awareness, it is urgently necessary to explore and develop shale gas resources. China is the third country after the United States and Canada to develop and utilize shale gas resources. To date, China has made significant progress in the research and development of shale gas [3–7]. In Jiaoshiba Chongqing, the first large-scale shale gas field in China was built and has reached 100 billion cubic meters [8].

Organic pores are widely developed in shale that is rich in organic material and are an important part of the shale reservoir space [9]. Shale gas can be stored in a free phase in organic pores and can be adsorbed onto the surface of

organic matter in an adsorbed phase [10]. The porosity of the organic matter directly determines the distribution of the gas [7]. The type and maturity of organic matter are the geological conditions used to judge the commercial developmental value of shale gas [11]. Therefore, the study of organic pores is important for shale gas research and the evaluation of shale gas as a resource.

There are many types of pores in shale. There are primary pores, such as matrix cracks and intergranular pores, and there are secondary pores, such as organic pores, dissolved pores, and organic microfractures [12]. Organic pores are important because they are one of the largest reservoir spaces. Organic pores have various shapes, and they can be elliptical, circular, or irregular polygons, but are primarily in the form of ellipses, with pore sizes between 5 and 200 nm [13–15]. Well-developed organic pores have good connectivity, forming interconnected pore networks that can contain large shale gas reservoirs. Pores in two adjacent organic materials or in different parts of the same organic material can be different [16, 17]. In addition, there are many forms of organic matter in shale, mainly occurring in the presence of clay and brittle minerals. Pores can comprise up to 50% of the volume of the organic matter. The formation of organic pores is a product of the maceral content of organic matter and the degree of host shale maturity. Some maceral generates hydrocarbons and a large number of pores as its maturity increases [18, 19]. When the maturity of the organic matter (R_o) is less than 0.90%, organic pores are not well developed. In the gas window, liquid hydrocarbons begin to crack, and organic pores begin to develop [20]. Loucks et al. [19] and Slatt et al. [12] indicated that organic pores formed when $R_o = 0.60\%$. The maturation of organic pores can be divided into three stages: the formation period ($0.60\% < R_o \leq 2.00\%$), the development period ($2.00\% < R_o \leq 3.50\%$), and the destruction period ($R_o > 3.50\%$). The density of organic pores is a function of the TOC content, maturity, and the type of organic matter such as maceral or pyrobitumen [21–23].

Currently, there is no detailed description or classification scheme for organic pores in shale. What characteristic differences may exist between different types of shale remains unclear. It is necessary to know the connectivity of organic pores in shale formations. In particular, the current understanding of the three-dimensional morphology and connectivity of pores in different types of organic matter is insufficient. Therefore, various organic pores in shale were analyzed to classify the types of organic matter present and the morphology and connectivity characteristics. The present study augments our understanding of shale gas storage space and will assist in the research and development of shale gas.

2. Geological Background

The Sichuan Basin is located at the northwestern edge of the Yangtze Platform [24]. The basin has experienced two stages: the Craton stage (from the Early Paleozoic to Middle Triassic) and the foreland basin stage (from the Late Triassic to Cenozoic) [25]. The Sichuan Basin began to form during the early Indosinian Movement and, eventually, formed a diamond-shaped sedimentary basin after the Himalayan movement (Figure 1). The Sichuan Basin is surrounded by a contiguous range of mountains. The Sichuan Basin is a complex, superimposed basin with terrestrial and marine sediments [26]. The shale deposits in the central Sichuan Basin are thin, and the shale deposits in the eastern, southeastern, and southwestern Sichuan Basin are relatively thick.

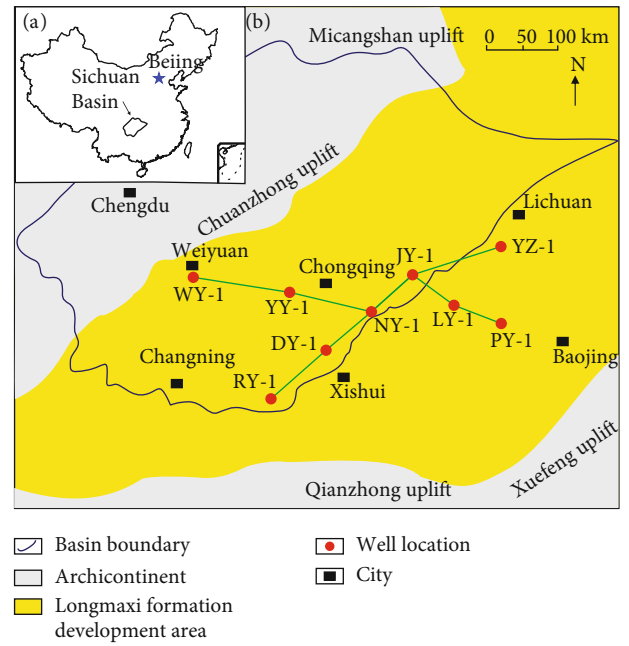

Figure 1: Tectonic setting and location of the southeast Sichuan Basin. (a) Location of the Sichuan Basin in China. (b) Tectonic setting of the southeast Sichuan Basin.

The southeast Sichuan Basin is composed mainly of ejective folds that consist of high-steep anticlines, loose synclines, and fault zones [26]. The basement of the southeast Sichuan Basin is composed of Presinian metamorphic rocks. The Devonian, Carboniferous, Cretaceous, and Paleogene rock strata were absent from the entire area. During the Early-Middle Ordovician, the area transformed from an open sea to a restricted sea surrounded by uplifts, resulting in a low-energy and anoxic sedimentary environment [27, 28]. During the Early Silurian, the southeastern Sichuan Basin was a semioccluded stagnant basin with a deep shelf environment. A black, organic-material-rich shale was deposited, forming the best layer for shale gas investigation in the region [29, 30].

The lower section of the Wufeng-Longmaxi Formation is primarily composed of a black graptolite shale, and the upper section is primarily a gray argillaceous siltstone [31]. During the Longmaxi's Formation period, the Sichuan Basin was shallow and has graptolite shale deposits and a short deposit range compared with that of the Wufeng's Formation period [32]. The Wufeng-Longmaxi Formation in the southeast Sichuan Basin is relatively thick, and the terrigenous detrital content increases from the lower to the upper section. At present, the Wufeng Formation and the lower Longmaxi Formation are the main shale gas reservoirs [33].

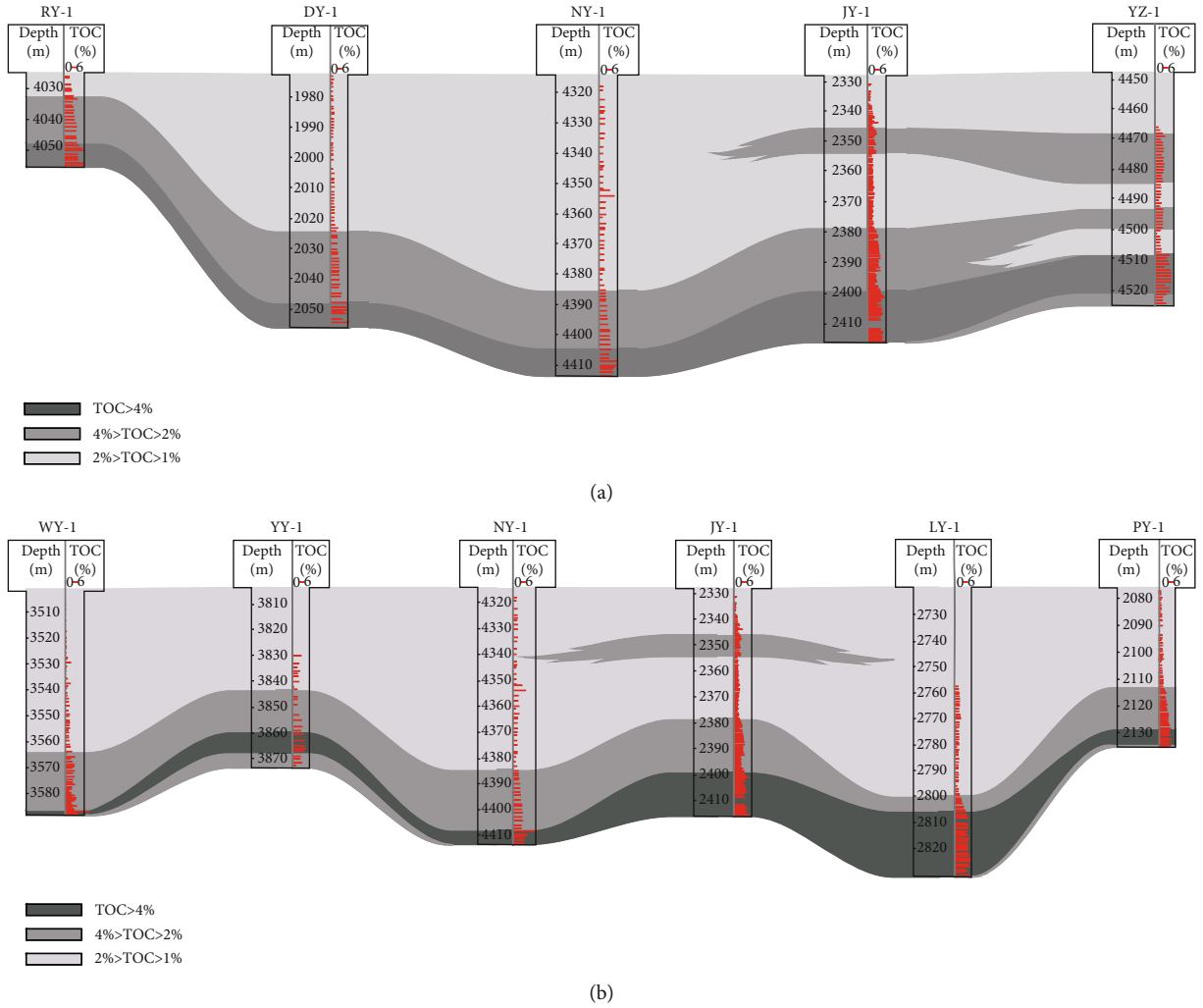

Figure 2: Comparison sections of the TOC content of the Wufeng-Longmaxi Formation shale in the southeast Sichuan Basin. (a) Section of the TOC content from northeast to southwest. (b) Section of the TOC content from east to west.

3. Sampling and Experimental Methods

The total organic carbon (TOC) content was tested with a Leco analyzer. The inorganic carbon in the sample was removed with diluted hydrochloric acid and then burned in a high-temperature oxygen oven to convert all the organic carbon to carbon dioxide. The TOC content was then measured by an infrared detector. The type and maturity of organic matter were observed under a LABORLUX 12 POL fluorescence microscope. Samples larger than 4 mm were cemented with a nonfluorescent cement to a microscope slide and observed using the microscopes oil immersion lens. A high-pressure mercury vapor or xenon lamp was used as the excitation source, and then, a blue or ultraviolet light was used to excite the filter. Organic matter with fluorescence was isolated and tested. The reflectance of the graptolite was determined. Then, the type and maturity of the organic material were obtained.

The two-dimensional micromorphology, structural characteristics, and three-dimensional connectivity of the samples were studied using an FEI Quanta 200F focused ion beam scanning electron microscope (FIB-SEM) in the high-vacuum scanning mode. The electron image was obtained from the secondary electron signal of the sample

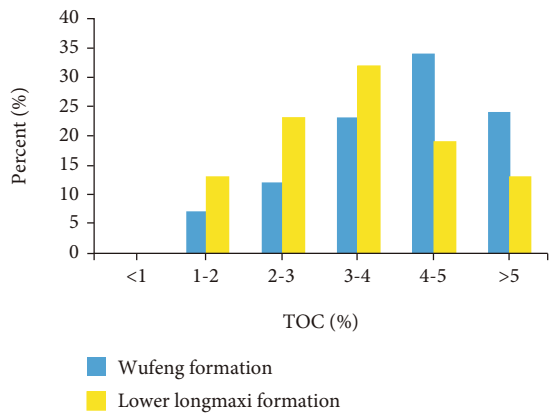

Figure 3: TOC distribution of the shale in the Wufeng-Longmaxi Formation at the southeast Sichuan Basin.

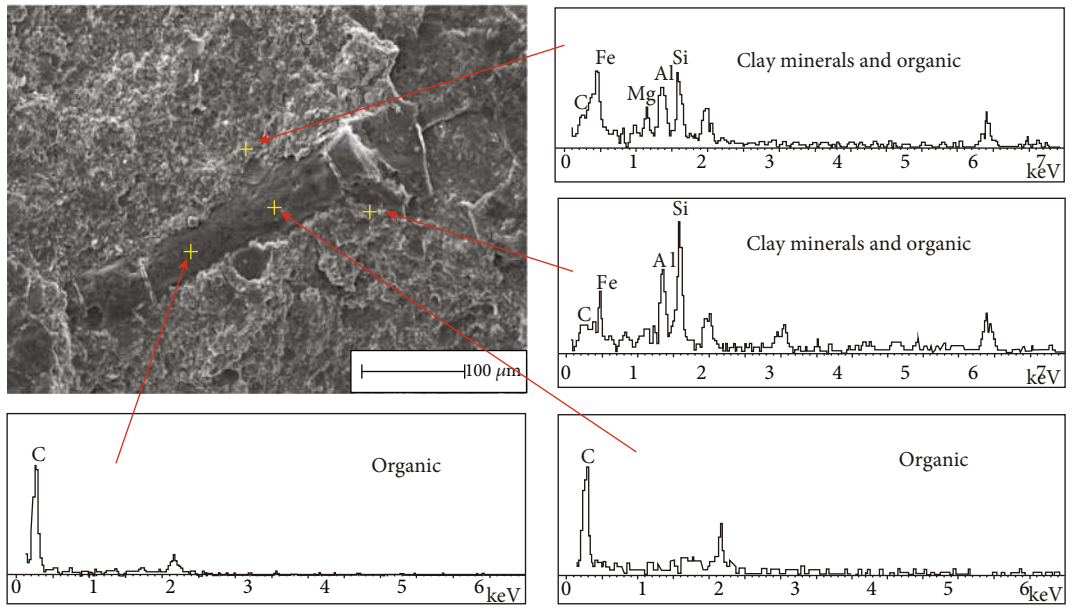

Figure 4: Graptolite photographs and energy spectrum of the Wufeng-Longmaxi Formation shale in the southeast Sichuan Basin. The fragment is graphitic, that is, mainly composed of carbon. The fragment is encased in clay minerals and carbonate minerals.

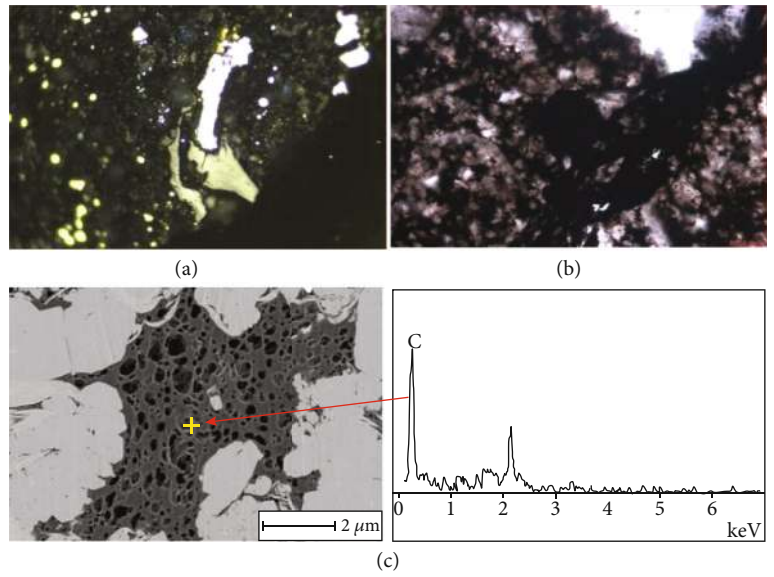

Figure 5: Pyrobitumen morphology photograph and energy spectrum of the Wufeng-Longmaxi Formation shale in the southeast Sichuan Basin. (a) Fluorescence microscope photo. (b) Polarized light microscope photo. (c) SEM photo and energy spectrum characteristics.

surface through an ion beam generated by a liquid metal (Ga) ion source. The sample was observed to have dimensions of 4.5 μm × 8 μm × 8 μm. The surface of the sample was polished with a JEOL IB-09010 argon ion sample polishing machine. Pores with apertures larger than 5 nm could be observed by the FIB-SEM, and ImageJ was used to calculate the face rate based on gray recognition.

A Zeiss Metrotom nano-CT was used to study the three-dimensional characteristics of the samples. Sixty-five micrometer diameter cylinder samples were selected. The resolution of the nano-CT in the present study was 65 nm. Therefore, pores lager than 65 nm could be imaged. The working principle is that the X-ray source and the detection receiver scan the samples synchronously. When each scan was completed, the scanning rack rotated to the next angle and then performed the next scan. Through digital image processing and three-dimensional reconstruction of the CT single-image and CT image sequences, the porosity of the samples was calculated, and an image was obtained of the three-dimensional distribution and connectivity of pores.

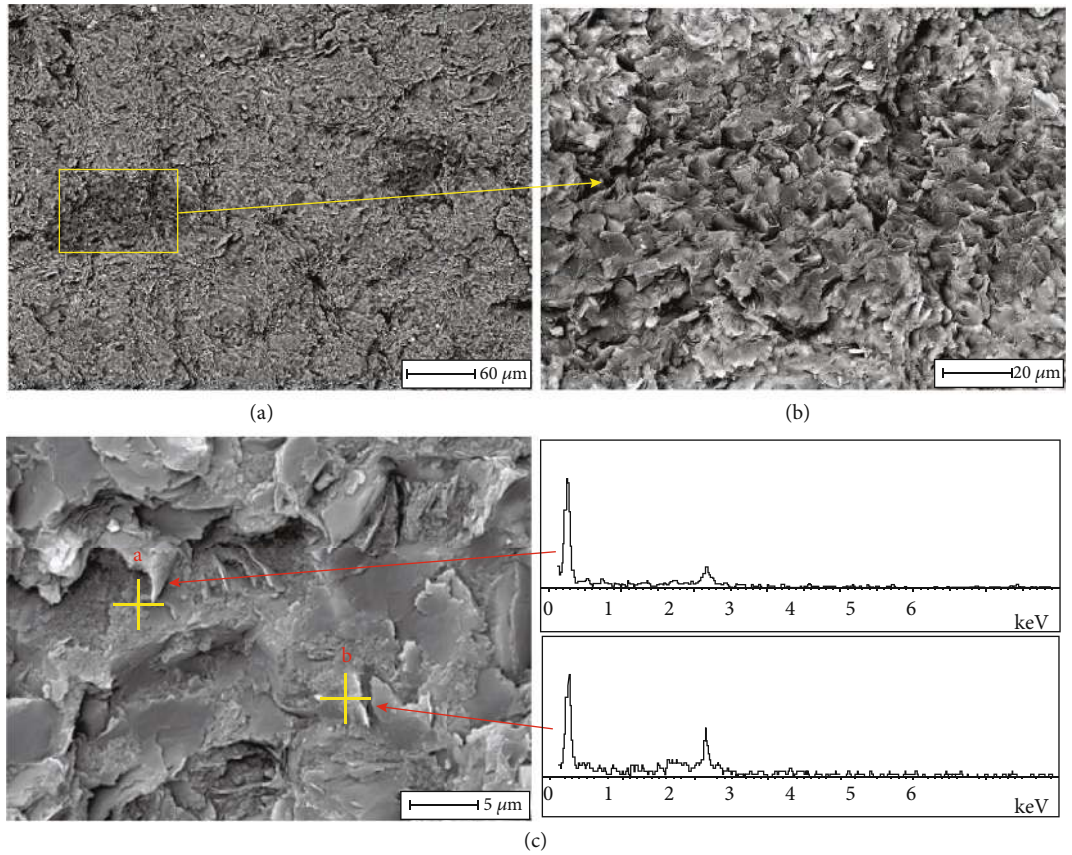

Figure 6: Algae morphological photograph and energy spectrum of the Wufeng-Longmaxi Formation shale in the southeast Sichuan Basin. (a) The dark part is algae. (b) Amplification of (a). (c) Amplification of (b). The algae are mainly carbonaceous and energy spectrum characteristics.

4. Results

4.1. Organic Matter Characteristics

4.1.1. Organic Matter Content. The organic matter in the southeast Sichuan Basin has many different characteristics in both the horizontal and vertical space [34]. The thickness of the TOC > 2% shale varies significantly from northeast to southwest (Figure 2(a)). From the northeast to the southwest, the thickness gradually declines. The thickest area is around the JY-1 well in the northeast, approximately 40 m thick, while the shale with TOC > 2% in the southwestern area is less than 20 m thick. The JY-1 well area and LY-1 well area have the thickest shale from east to west (Figure 2(b)). In the vertical direction, the TOC > 4% shale is mainly concentrated at the Wufeng Formation and at the bottom of the Longmaxi Formation, and the TOC content gradually decreases from the bottom to the top in the Longmaxi Formation. The average TOC content of the Wufeng Formation is 4.3%, while the average TOC content of the bottom of the Longmaxi Formation is 3.2% (Figure 3).

4.1.2. Organic Matter Type. Based on light microscopy and FIB-SEM observations, the majority of organic matter in the southeast Sichuan Basin is algae, pyrobitumen, and graptolite. A small amount of biodetritus was also observed, such as acritarchs, chitinozoans, and sponge spicules (Figures 4–6). Most of the graptolite has a thin, dense carbonaceous structure (Figure 4), and its pores are poorly developed. There are contraction fractures between the graptolite and surrounding minerals. Energy spectrum analysis showed that the graptolite is mainly carbonaceous.

Pyrobitumen generally fills the space between mineral particles and has no fixed form (Figure 5). Compared with the dense structure of graptolite, pyrobitumen has a loose structure and more well-developed pores (Figure 5(c)). Energy spectrum analysis showed that the main elemental composition of pyrobitumen is also carbonaceous (Figure 5(d)).

Algae are generally secondary components that postdate hydrocarbon generation and are covered with lamellate clay minerals. The clay minerals do not have a fixed orientation and look like petals (Figure 6). The algae are also relatively loose, and energy spectrum analysis showed that the elemental composition of the algae is mainly carbonaceous (Figure 6(c)).

Energy spectrum analysis showed that the biodetritus contains mostly phosphorus and calcium, with a relatively complete structure and morphology (Figure 7; [35]). The biodetritus is relatively dense, and its pores are either not developed or only a few nanoscale micropores are developed.

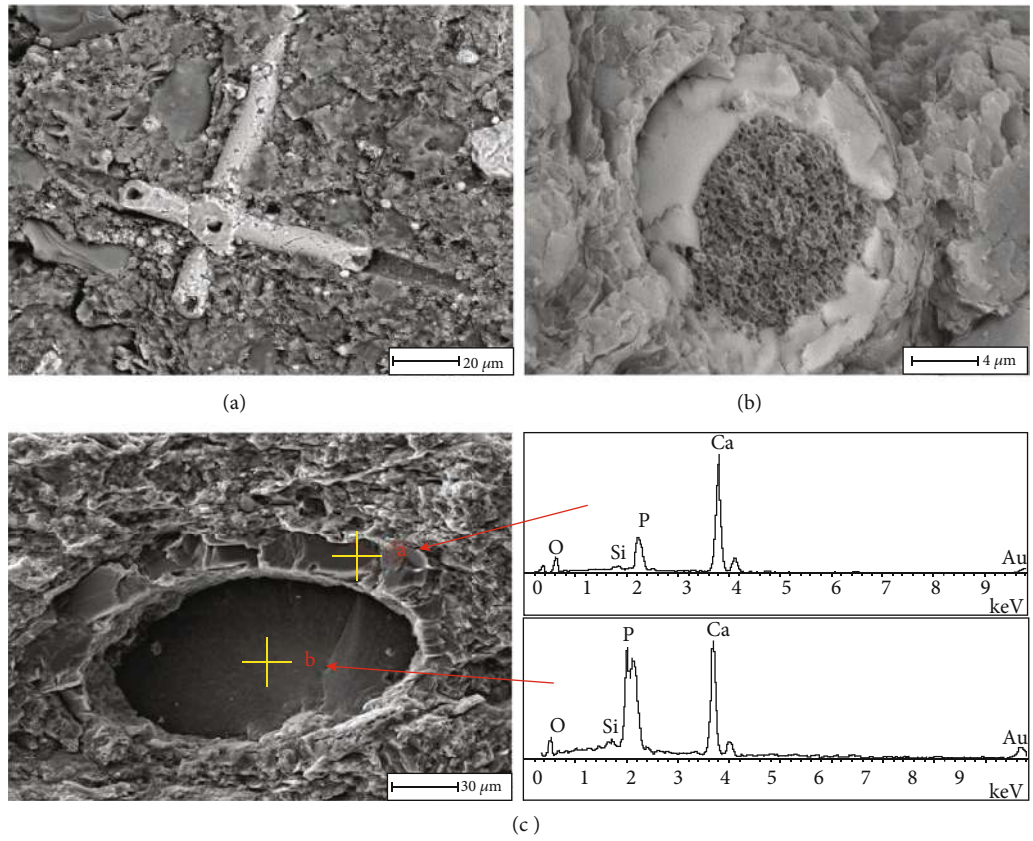

Figure 7: Biodetritus morphology photograph and energy spectrum of the Wufeng-Longmaxi Formation shale in the southeast Sichuan Basin. (a) Sponge spicule. (b) Sponge spicule (cross section). (c) Biodetritus with calcium and phosphorus.

4.1.3. Organic Matter Maturity. The microscopic organic components that indicate the maturity of the black shale in the Wufeng-Longmaxi Formation in the southeast Sichuan Basin are mainly three types: pyrobitumen, biodetritus (predominantly graptolite), and vitrinite-like maceral (VLM). The black shale of the Wufeng-Longmaxi Formation is abundant in graptolite, with obvious morphological features. In the present study, the reflectance of the graptolite was measured. Based on 18 samples from 12 wells, the R_o is between 2.22% and 3.13%, with an average of 2.71% [36, 37], indicating that the shale has a high degree of maturity (Figure 8).

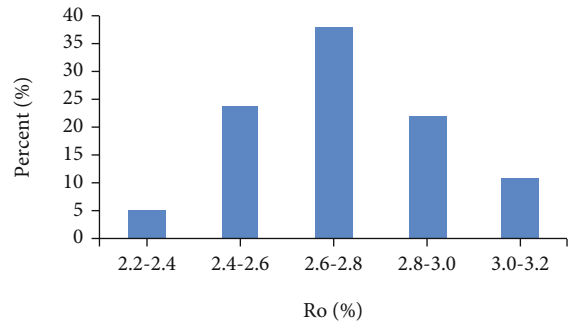

Figure 8: Equivalent vitrinite reflectance distribution of the Wufeng-Longmaxi Formation shale in the southeast Sichuan Basin.

4.2. Organic Pore Characteristics

4.2.1. Algae Pores. The pores in the organic matter of the Wufeng-Longmaxi Formation shale are generally well developed, but the pores in different types of organic matter show significant variability. The cell structure of the algae is poorly preserved, and most of it have been degraded and heavily micronized. This type of organic matter has a distinct shape, and the inorganic minerals produced by the internal metasomatism have an obvious biological structure. The organic matter pores inside the algae mostly have a local concentration, and the surface porosity is approximately 15% (Figure 9).

4.2.2. Graptolite Pores. Generally, graptolite is poorly preserved and displays a fixed, rigid shape. Fractures can form between the graptolite and inorganic minerals. Small quantities of inorganic minerals are observed inside the graptolite, and the pores are poorly developed, with 5% surface porosity (Figure 10).

4.2.3. Pyrobitumen Pores. Pyrobitumen does not have a fixed shape and fills the spaces in the inorganic mineral particles of the clay layers. The pores are well developed in the pyrobitumen, with a 30% surface porosity (Figure 11). The pore shape within the pyrobitumen is controlled by the morphology of the pyrobitumen. The pores are mainly concentrated in the center of the pyrobitumen. The pore morphology is mostly

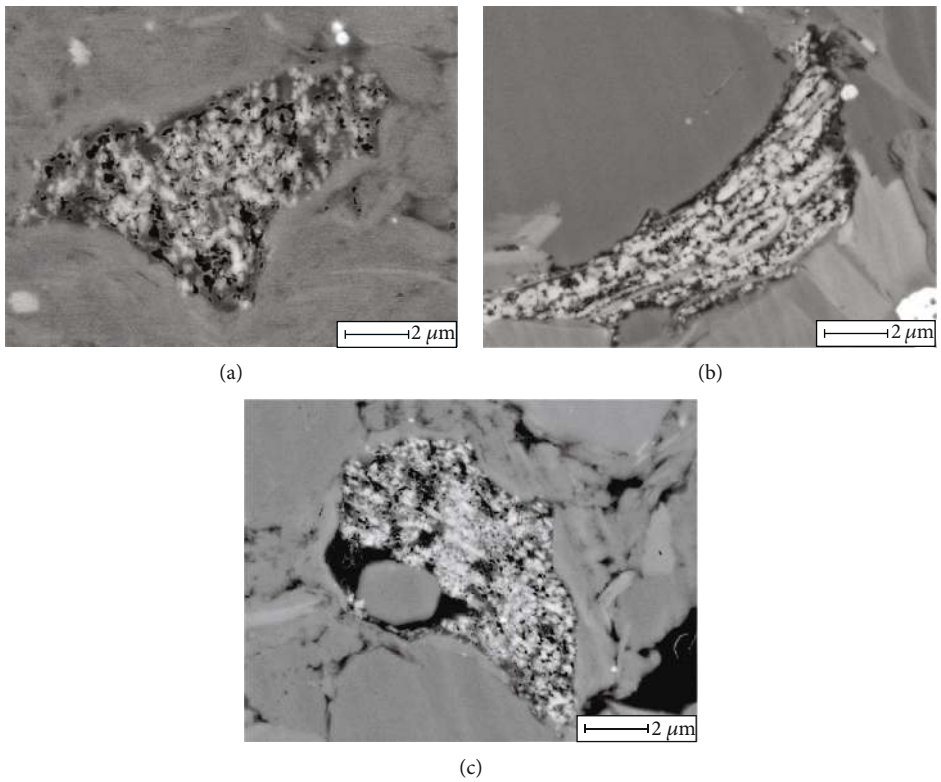

(a) (b)

(c)

Figure 9: Pore characteristics of the algae in the Wufeng-Longmaxi Formation shale at the southeast Sichuan Basin.

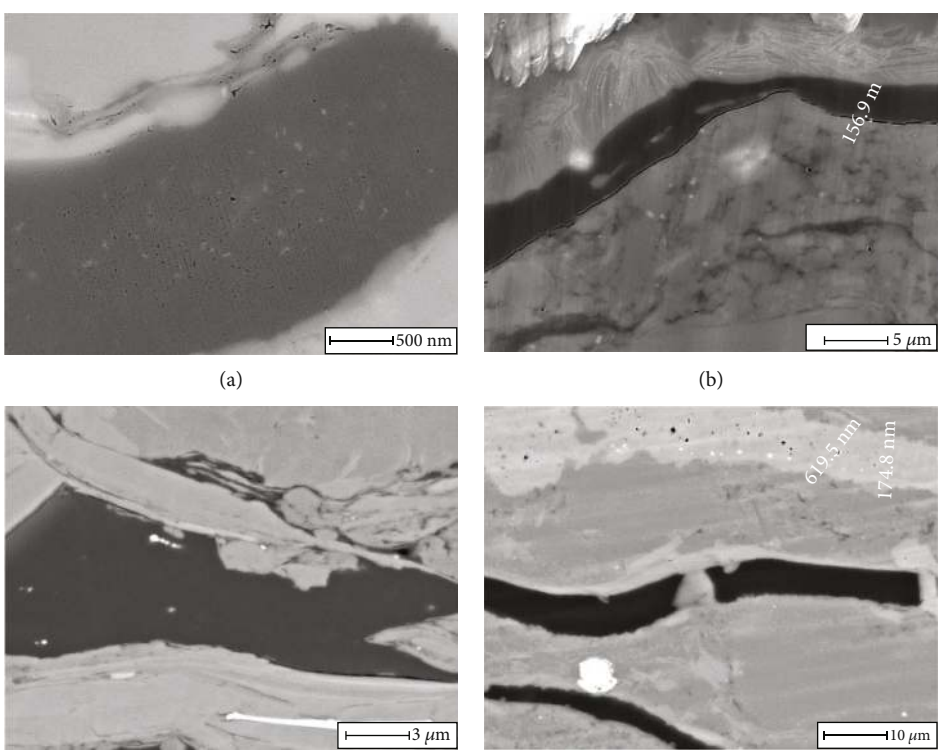

(a) (b)

(c) (d)

Figure 10: The pore characteristics of graptolite in the Wufeng-Longmaxi Formation shale at the southeast Sichuan Basin.

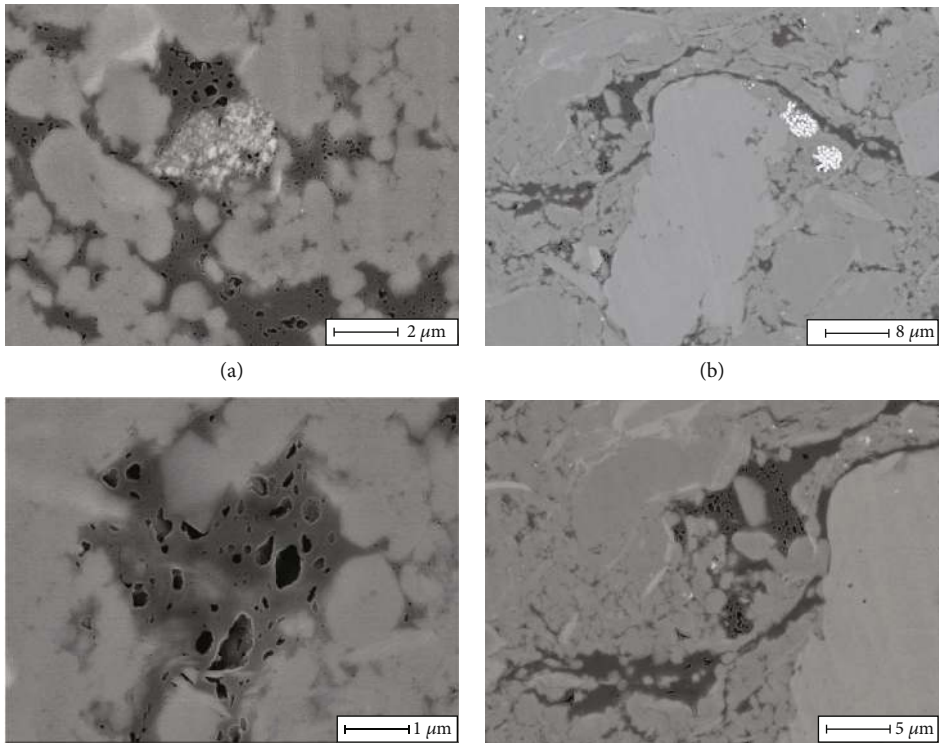

(a) (b) (c) (d)

Figure 11: The pore characteristics of pyrobitumen in the Wufeng-Longmaxi Formation shale at the southeast Sichuan Basin.

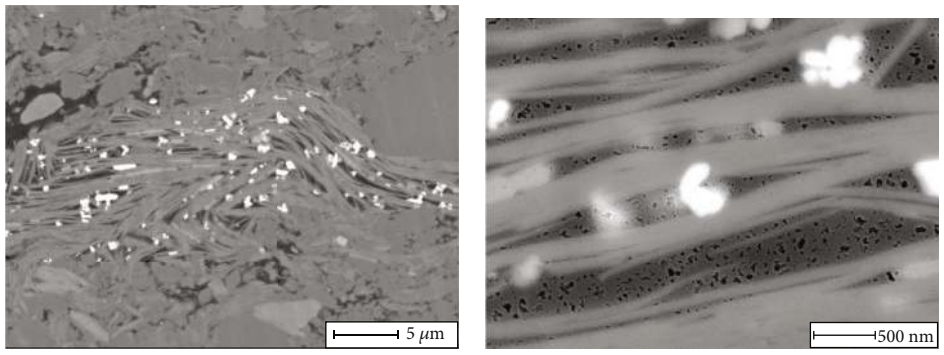

(a) (b)

Figure 12: Pyrobitumen in the clay mineral layers, with pores mainly smaller than 50 nm.

ellipsoidal or semiround, with a 10-300 nm long axis and a 2-100 nm short axis. The pores are less developed at the edges of the pyrobitumen, especially at the throat area adjacent to the inorganic minerals. The morphology of the pyrobitumen is mainly long strips or flat, with an aspect ratio greater than 5 : 1. The long axis direction of the pores agrees with the long axis direction of the pyrobitumen (Figure 11). The pyrobitumen portion contained pores ranging in size from 5 to 50 nm (Figure 12; [38]). These pyrobitumen pores are the main body of organic pores in the Wufeng-Longmaxi Formation shale.

5. Discussion

5.1. Morphology and Connectivity of Organic Pores. The pores in the shale exist in three dimensions. Nano-CT scans can display the internal mineral composition and pore structure in 3D [39]. The connectivity of the organic-material-rich shale at the bottom of the Wufeng-Longmaxi Formation is medium-poor, and the pore size is small (Figure 13). The continuity of organic matter in three-dimensional space is good, and a large number of pores have developed in these well-connected organic materials. Figure 13(b) shows the organic pores in different regions using multiple colors. Areas with the same color indicate that the nanopores in the organic matter of this part are connected. These different-sized pores form a complex spatial network structure. The pores in the sample are mainly circular, and the shape of the pores is sill-like, sheet-like, and tubular, with moderate connectivity. The throat is needle-shaped and partially sill-like (Figure 13(c)). The sample had a total of more

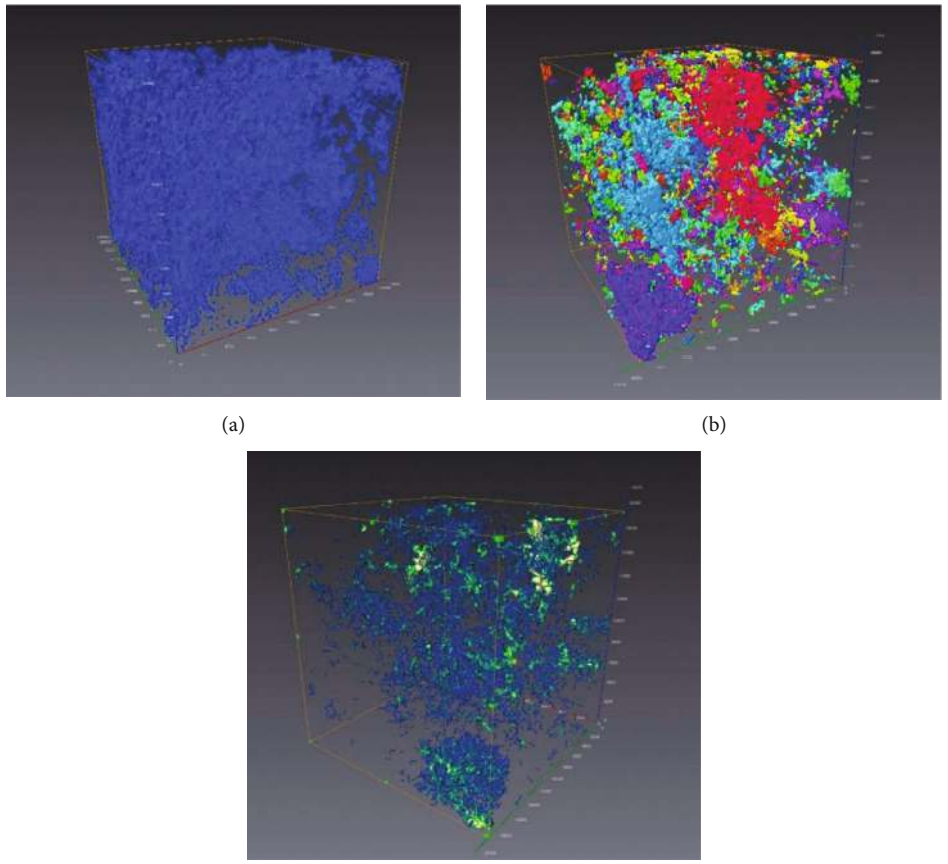

(a) (b) (c)

Figure 13: Organic pore characteristics of the organic-material-rich shale based on nano-CT. The TOC is 5.7%. (a) The blue part is organic matter. (b) Interconnected pores in the organic matter. (c) Throat distribution in the organic matter.

than 7400 organic pores, with a total volume of 4.6×10^{11} nm^3, which accounted for 5.7% of the total sample volume of 8×10^{12} nm^3. The sample had 5120 organic pores (larger than 65 nm), and the total volume of the organic pores was 2.6×10^{11} nm^3, which accounted for 3% of the total volume of the sample and 56.6% of the total organic matter volume.

The organic-material-poor shale in the middle and upper parts of the Wufeng-Longmaxi Formation has poor connectivity (Figure 14). The continuity of the organic matter in three-dimensional space is poor, and the connected organic pore range is obviously reduced (Figure 14(b)). The same characteristics are also visible in the organic throat distribution. The pores of the sample were mainly elongated (similar to intergranular pores) and flake-shaped with poor connectivity. The throat was needle-shaped (Figure 14(c)). The sample had a total of 2698 organic pores with an overall volume of 1.2×10^{11} nm^3, which accounted for approximately 1.6% of the total sample volume of 8×10^{12} nm^3. The sample had 1067 organic pores, which accounted for 0.9% of the total volume of the sample.

According to the 3D FIB-SEM data, the organic pores in the Wufeng-Longmaxi Formation shale with long axes < 100 nm accounted for approximately 89% of the total organic pores, while the organic pores with long axes > 200 nm accounted for less than 4% of the total organic pores (Figure 15). Organic pores have a relatively high proportion of small pores [40]. It was determined that the majority of the organic pores in the sample were less than 50 nm, and a large number of the small pores had developed inside the organic matter.

The organic pores with aspect (long – to – minor axis) ratios > 4 only comprise approximately 15% of the total organic pores, and more than 50% of the pores have aspect ratios < 2 (Figure 16). The morphological characteristics of the organic pores obtained by three-dimensional FIB-SEM are similar to those obtained by two-dimensional FIB-SEM: the shapes of the organic pores are primarily rounded, nearly circular, or elliptical.

5.2. Role of Pyrobitumen Pores. The majority of organic matter in the Wufeng-Longmaxi shale are migrated organic matter of amorphous form, uniform color, and nanometer-scale internal pores [41]. The migrated organic matter was injected into the mineral pores (mainly intergranular) in the form of liquid hydrocarbon during the shale oil generation stage [42]. If the TOC content in the shale is 5% by weight, the organic matter density is approximately 50% of the shale density. The organic matter then accounts for nearly 10% of the pore volume of the shale, while the organic matter contains approximately 20%-40% of the

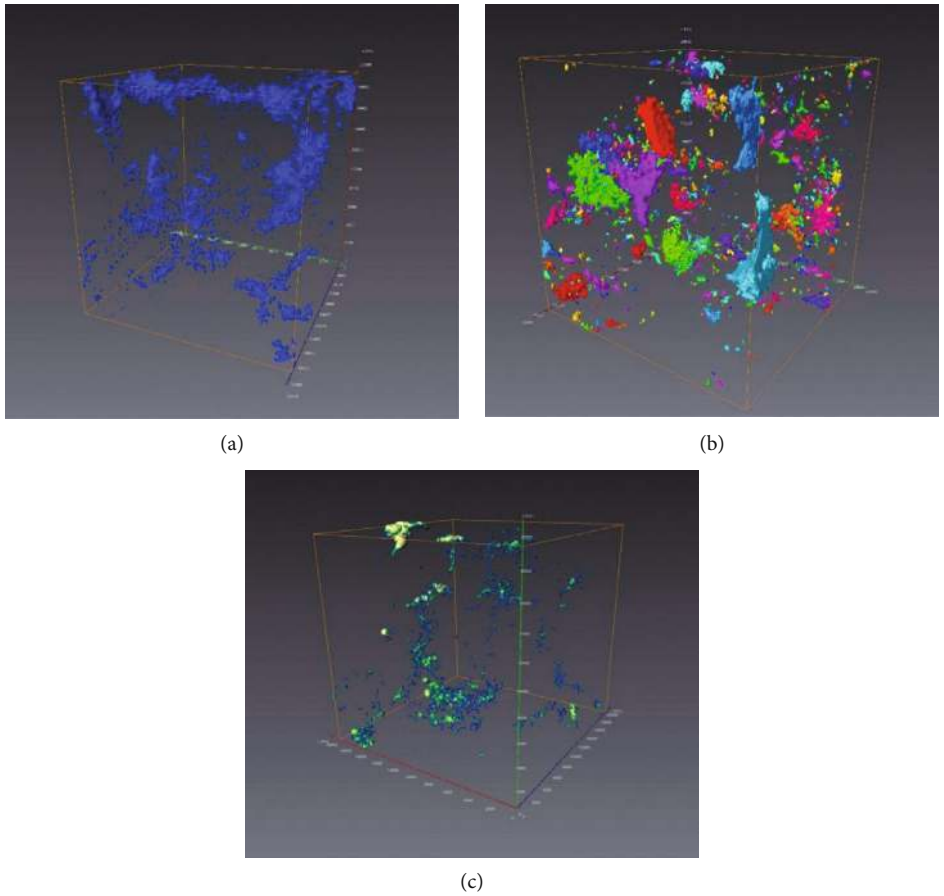

Figure 14: Organic pore characteristics of the shale based on the nano-CT. TOC is 1.6%. (a) The blue part is organic matter. (b) Interconnected pores in the organic matter. (c) Throat distribution in the organic matter.

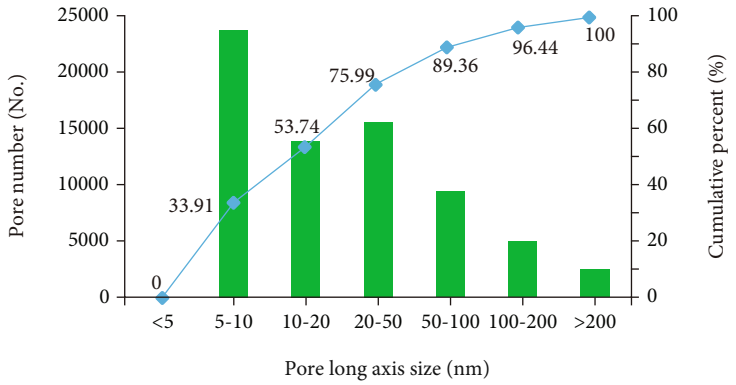

Figure 15: Characteristics of the long axis of organic pores based on 3D FIB-SEM data. The majority of long axes are shorter than 100 nm.

volume occupied by organic pores. Therefore, the organic matter has an organic matter porosity of 2%-4% of the total volume of the shale. Due to its low porosity and poor permeability, it was difficult for liquid hydrocarbon to migrate out of the shale [43]. The remaining hydrocarbon separated into light hydrocarbon (primarily methane) and heavy hydrocarbon (primarily solid pyrobitumen) [44]. The pyrobitumen pores were formed during the process of gas and liquid separation.

Based on the analysis of 832 pyrobitumen enclaves in 16 samples, it was determined that the pyrobitumen pores are primarily ellipsoidal or near-circular. The long-to-minor axis ratios of the pyrobitumen pores are similar. The aspect ratios are concentrated at <3, and less than 10% of the long-to-minor axis ratios are >3 (Figure 17).

The pores in the center of the pyrobitumen are mostly rounded, and the aspect ratios are concentrate close to 1. The pores close to the throat between inorganic minerals

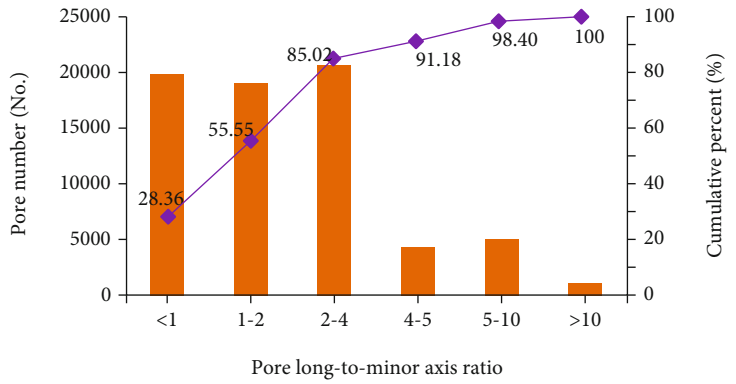

Figure 16: Characteristics of the aspect ratio of the organic pores based on 3D FIB-SEM data.

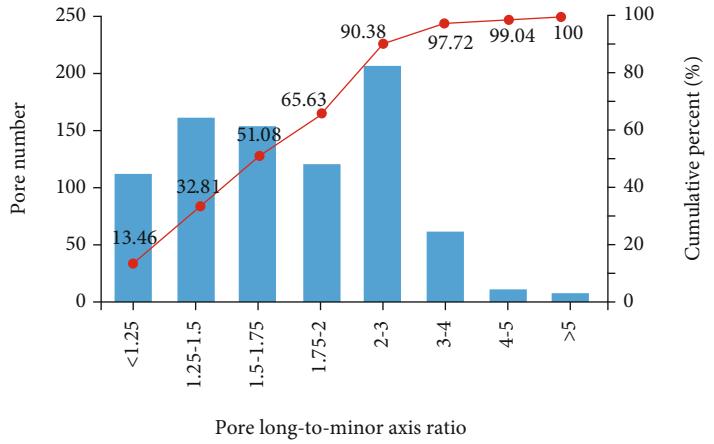

Figure 17: Characteristics of the aspect ratios of the pyrobitumen pores based on 2D FIB-SEM data.

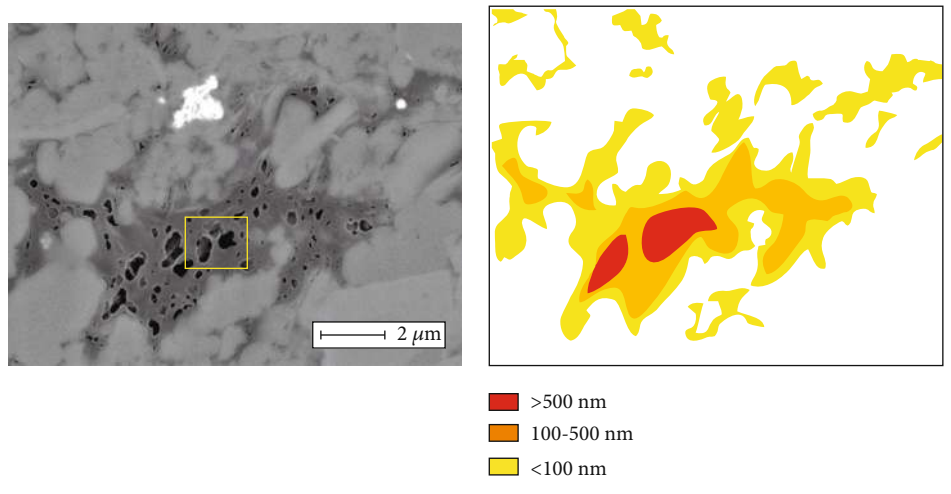

Figure 18: Characteristics of the pyrobitumen pores based on 2D FIB-SEM data. (a) The large pores are concentrated at the center of the pyrobitumen. (b) Pattern of figure (a).

are flat shaped or in long strips for the most part, with long-to-minor axis ratios higher than 3. The larger the volume of a single pyrobitumen enclave, the more developed the pyrobitumen pores and the larger the pore size. Additionally, the large pores are concentrated at the center of the pyrobitumen (Figure 18).

For example, Figure 18(a) shows that one 9 μm long pyrobitumen portion has abundant nanopores, and its surface

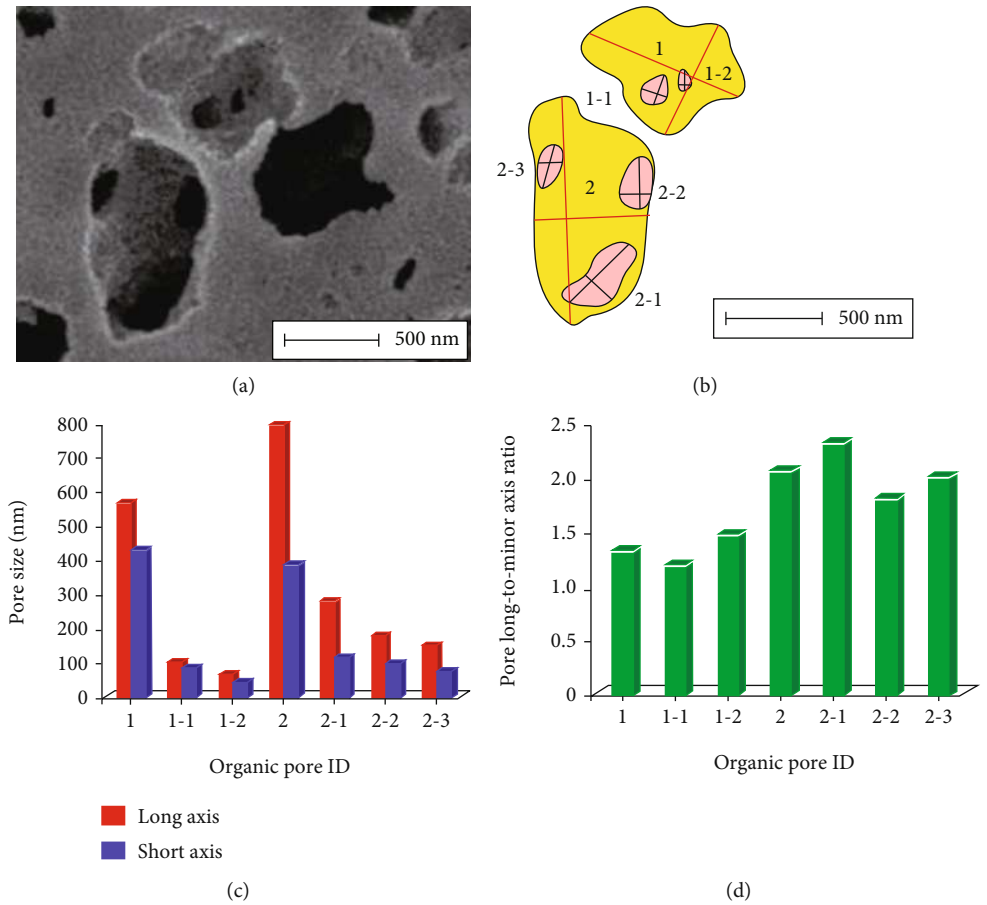

Figure 19: Pores in the pyrobitumen based on 2D FIB-SEM data. (a) Magnification of Figure 18(a) showing good pore connectivity. (b) Pattern of figure (a). (c) Statistics of the long axis and short axis of pyrobitumen pores. (d) Proportional distribution of the long and short axes of pyrobitumen pores.

porosity is approximately 30% (Figure 18(a)). From the edge of the pyrobitumen to the center, the size of the pores has a pronounced increasing trend, from a majority of less than 100 nm near the edge, increasing to 500 nm further in, and increasing to greater than 500 nm at the center of the pyrobitumen. This trend may indicate that most of the gas are generated at the center of the organic matter concentrations (Figure 18(b)). The long axis direction of the pores is generally coordinated with the extension direction of the pyrobitumen. Especially in narrow pyrobitumen enclaves, the long axis direction of the pores is consistent with the extension direction of the pyrobitumen, indicating that pyrobitumen deformation has occurred on the internal pyrobitumen pores.

The pyrobitumen pores are not completely isolated from each other and have good connectivity. The large pores are generally interconnected by small pores (Figure 19(a)). In the No.1 pore, there are 2 secondary nanopores, and their aspect ratios are all lower than 1.5 (Figures 19(b)–19(d)). In the No.2 pore, there are 3 secondary nanopores, and their aspect ratios are all greater than 1.5 (Figures 19(b)–19(d)). The relationship between the large pyrobitumen pores and the secondary pyrobitumen pores indicates that they were generated by similar processes. During the formation and accumulation of shale gas, small secondary pores may accumulate within large pores, increasing the size of the larger pores.

6. Conclusion

The distribution of organic matter in the southeast Sichuan Basin has distinct variations both horizontally and vertically. The TOC > 4% shale is mainly concentrated at the Wufeng Formation and at the bottom of the Longmaxi Formation. The organic materials are primarily algae (secondary components), pyrobitumen, and graptolite, with a small amount of biodetritus, such as acritarch, chitinozoa, and sponge spicule. The Wufeng-Longmaxi Formation shale has a high degree of thermal evolution, and its R_o is between 2.22% and 3.13%, with an average of 2.71%.

There are three main types of organic pores: algae pores, graptolite pores, and pyrobitumen pores. The cell structure of algae pores is poorly preserved but displays an apparent biological structure. Algae pores are locally concentrated. Graptolite is generally poorly preserved and has a fixed, rigid shape. Small quantities of inorganic minerals can be found inside the graptolite. The pyrobitumen does not have a fixed shape and fills the spaces between inorganic mineral particles and clay layers. The pyrobitumen pores are well developed, as determined by the overall morphology of the pyrobitumen enclaves.

The pores in the organic-material-rich shale are primarily circular, nanoscale pores. The majority of throats are

needle shaped, and the organic pores may account for more than 50% of the total organic matter volume. The organic matter in the organic-material-poor shale has poor continuity in three-dimensional space. The pores are mostly long and narrow, and the majority of throats are needle shaped. The organic pores may account for less than 1% of the total sample volume.

The majority of the pyrobitumen pores are ellipsoidal or near-circular, with aspect ratios concentrated at <3. The pores in the center of the pyrobitumen are mostly rounded, and the aspect ratios are predominantly close to 1. The pores close to the throat between the inorganic minerals are largely flat or in the shape of long strips, and their aspect ratios are mostly greater than 3. The large pores are concentrated in the center of the pyrobitumen, and the pyrobitumen pores are generally well connected.

Data Availability

The experimental data used to support the findings of this study are included within the manuscript.

Conflicts of Interest

The authors' declare that they have no conflicts of interest.

Acknowledgments

This study was supported by the National Natural Science Foundation of China (Grant No. 41872124) and the National Science and Technology Major Project (No. 2017ZX05036004). Thanks are due to Guangxiang Liu, Bo Gao, Haikuan Nie, Quanyou Liu, Tong Zhu, Ruyue Wang, and Pengwei Wang who participate in the project and give much critical suggestion and help on the thesis. We sincerely appreciate all anonymous reviewers and the handling editor for their critical comments and constructive suggestions.

References

[1] A. Vengosh, R. B. Jackson, N. Warner, T. H. Darrah, and A. Kondash, "A critical review of the risks to water resources from unconventional shale gas development and hydraulic fracturing in the United States," *Environmental Science & Technology*, vol. 48, no. 15, pp. 8334–8348, 2014.

[2] S. Balasubramanian, P. Chen, and S. Bose, "Recent advances in enhanced oil recovery technologies for unconventional oil reservoirs," *Paper presented at the Offshore Technology Conference*, 2018, Houston, TX, USA, April 2018, 2018.

[3] C. Han, Z. Jiang, M. Han, M. Wu, and W. Lin, "The lithofacies and reservoir characteristics of the Upper Ordovician and Lower Silurian black shale in the Southern Sichuan Basin and its periphery, China," *Marine and Petroleum Geology*, vol. 75, pp. 181–191, 2016.

[4] T. Jiang, Z. Jin, G. Liu et al., "Source analysis of siliceous minerals and uranium in early Cambrian shales, South China: Significance for shale gas exploration," *Marine and Petroleum Geology*, vol. 102, pp. 101–108, 2019.

[5] X. Qiu, C. Liu, G. Mao, Y. Deng, F. Wang, and J. Wang, "Major, trace and platinum-group element geochemistry of the Upper Triassic nonmarine hot shales in the Ordos basin, Central China," *Applied Geochemistry*, vol. 53, pp. 42–52, 2015.

[6] J. Wu, C. Liang, Z. Jiang, and C. Zhang, "Shale reservoir characterization and control factors on gas accumulation of the lower Cambrian Niutitang shale, Sichuan Basin," *Geological Journal*, vol. 54, no. 3, pp. 1604–1616, 2018.

[7] K. Zhang, J. Peng, W. Liu et al., "The role of deep geofluids in the enrichment of sedimentary organic matter: a case study of the late Ordovician-Early Silurian in the upper Yangtze region and early Cambrian in the lower Yangtze region, South China," *Geofluids*, vol. 2020, Article ID 8868638, 12 pages, 2020.

[8] Z. He, Z. Hu, H. Nie, S. Li, and J. Xu, "Characterization of shale gas enrichment in the Wufeng Formation-Longmaxi Formation in the Sichuan Basin of China and evaluation of its geological construction-transformation evolution sequence," *Journal of Natural Gas Geoscience*, vol. 2, no. 1, pp. 1–10, 2017.

[9] F. Wang and R. M. Reed, "Pore networks and fluid flow in gas shales," in *SPE Annual Technical Conference and Exhibition*, New Orleans, LA, USA, October 2009.

[10] T. Zhang, G. S. Ellis, S. C. Ruppel, K. Milliken, and R. Yang, "Effect of organic-matter type and thermal maturity on methane adsorption in shale-gas systems," *Organic Geochemistry*, vol. 47, pp. 120–131, 2012.

[11] S. Chen, Y. Zhu, H. Wang, H. Liu, W. Wei, and J. Fang, "Shale gas reservoir characterisation: a typical case in the southern Sichuan Basin of China," *Energy*, vol. 36, no. 11, pp. 6609–6616, 2011.

[12] R. M. Slatt and N. R. O'Brien, "Pore types in the Barnett and Woodford gas shales: contribution to understanding gas storage and migration pathways in fine-grained rocks," *AAPG Bulletin*, vol. 95, no. 12, pp. 2017–2030, 2011.

[13] M. E. Curtis, C. H. Sondergeld, R. J. Ambrose, and C. S. Rai, "Microstructural investigation of gas shales in two and three dimensions using nanometer-scale resolution imaging," *AAPG Bulletin*, vol. 96, no. 4, pp. 665–677, 2012.

[14] X. Tang, Z. Jiang, Z. Li et al., "The effect of the variation in material composition on the heterogeneous pore structure of high-maturity shale of the Silurian Longmaxi formation in the southeastern Sichuan Basin, China," *Journal of Natural Gas Science and Engineering*, vol. 23, pp. 464–473, 2015.

[15] F. Yang, Z. Ning, D. Kong, and H. Liu, "Pore structure of shales from high pressure mercury injection and nitrogen adsorption method," *Natural Gas Geoscience*, vol. 24, no. 3, pp. 450–455, 2013.

[16] G. R. Chalmers, R. M. Bustin, and I. M. Power, "Characterization of gas shale pore systems by porosimetry, pycnometry, surface area, and field emission scanning electron microscopy/transmission electron microscopy image analyses: examples from the Barnett, Woodford, Haynesville, Marcellus, and Doig units," *AAPG Bulletin*, vol. 96, no. 6, pp. 1099–1119, 2012.

[17] H. Tian, L. Pan, T. Zhang, X. Xiao, Z. Meng, and B. Huang, "Pore characterization of organic-rich Lower Cambrian shales in Qiannan Depression of Guizhou Province, Southwestern China," *Marine and Petroleum Geology*, vol. 62, pp. 28–43, 2015.

[18] D. M. Jarvie, R. J. Hill, T. E. Ruble, and R. M. Pollastro, "Unconventional shale-gas systems: the Mississippian Barnett shale of north-Central Texas as one model for thermogenic

shale-gas assessment," *AAPG Bulletin*, vol. 91, no. 4, pp. 475–499, 2007.

[19] R. G. Loucks, R. M. Reed, S. C. Ruppel, and D. M. Jarvie, "Morphology, genesis, and distribution of nanometer-scale pores in siliceous mudstones of the Mississippian Barnett shale," *Journal of Sedimentary Research*, vol. 79, no. 12, pp. 848–861, 2009.

[20] M. E. Curtis, C. H. Sondergeld, and C. S. Rai, *Relationship between or- ganic shale microstructure and hydrocarbon generation*, Society of Petroleum Engineers, The Woodlands, TX, USA, 2013.

[21] T. Cao, Z. Song, S. Wang, and J. Xia, "Characterization of pore structure and fractal dimension of Paleozoic shales from the northeastern Sichuan Basin, China," *Journal of Natural Gas Science and Engineering*, vol. 35, pp. 882–895, 2016.

[22] X. Liang, T. Zhang, Y. Yang et al., "Microscopic pore structure and its controlling factors of overmature shale in the lower Cambrian Qiongzhusi Fm, northern Yunnan and Guizhou provinces of China," *Natural Gas Industry*, vol. 34, no. 2, pp. 18–26, 2014.

[23] K. Zhang, J. Peng, X. Wang et al., "Effect of organic maturity on shale gas genesis and pores development: a case study on marine shale in the upper Yangtze region, South China," *Open Geosciences*, vol. 12, no. 1, pp. 1617–1629, 2020.

[24] C. Zou, J. Du, C. Xu et al., "Formation, distribution, resource potential, and discovery of Sinian-Cambrian giant gas field, Sichuan Basin, SW China," *Petroleum Exploration and Development*, vol. 41, no. 3, pp. 306–325, 2014.

[25] S. Chen, C. J. L. Wilson, and B. A. Worley, "Tectonic transition from the Songpan-Garzê Fold Belt to the Sichuan Basin, southwestern China," *Basin Research*, vol. 7, no. 3, pp. 235–253, 1995.

[26] T. Guo, "Evaluation of highly thermally mature shale-gas reservoirs in complex structural parts of the Sichuan Basin," *Journal of Earth Science*, vol. 24, no. 6, pp. 863–873, 2013.

[27] T. Guo and H. Zhang, "Formation and enrichment mode of Jiaoshiba shale gas field, Sichuan Basin," *Petroleum Exploration and Development*, vol. 41, no. 1, pp. 31–40, 2014.

[28] C. Liang, Z. Jiang, Y. Cao, J. Zhang, and L. Guo, "Sedimentary characteristics and paleoenvironment of shale in the Wufeng-Longmaxi Formation, North Guizhou Province, and its shale gas potential," *Journal of Earth Science*, vol. 28, no. 6, pp. 1020–1031, 2017.

[29] J. Wu, C. Liang, Z. Hu et al., "Sedimentation mechanisms and enrichment of organic matter in the Ordovician Wufeng Formation-Silurian Longmaxi formation in the Sichuan Basin," *Marine and Petroleum Geology*, vol. 101, pp. 556–565, 2018.

[30] C. Zou, D. Dong, S. Wang et al., "Geological characteristics and resource potential of shale gas in China," *Petroleum Exploration and Development*, vol. 37, no. 6, pp. 641–653, 2010.

[31] Z. Jiang, L. Guo, and C. Liang, "Lithofacies and sedimentary characteristics of the Silurian Longmaxi shale in the southeastern Sichuan Basin, China," *Journal of Palaeogeography*, vol. 2, no. 3, pp. 238–251, 2013.

[32] S. Liu, W. Ma, L. Jansa, W. Huang, X. Zeng, and C. Zhang, "Characteristics of the shale gas reservoir rocks in the lower silurian longmaxi formation, East Sichuan basin, China," *Energy Exploration & Exploitation*, vol. 31, no. 2, pp. 187–219, 2013.

[33] C. Zou, D. Dong, Y. Wang et al., "Shale gas in China: characteristics, challenges and prospects (II)," *Petroleum Exploration and Development*, vol. 43, no. 2, pp. 182–196, 2016.

[34] J. Liu, Y. Yao, D. Elsworth, D. Liu, Y. Cai, and L. Dong, "Vertical heterogeneity of the shale reservoir in the lower Silurian Longmaxi Formation: analogy between the southeastern and northeastern Sichuan Basin, SW China," *Minerals*, vol. 7, no. 8, p. 151, 2017.

[35] H. K. Nie, Z. J. Jin, and J. C. Zhang, "Characteristics of three organic matter pore types in the Wufeng-Longmaxi Shale of the Sichuan Basin, Southwest China," *Southwest China. Scientific Reports*, vol. 8, no. 1, article 7014, 2018.

[36] C. Cao, Q. Shang, and Y. Fang, "The study of graptolite reflectance as the indicator of source rock maturation in Ordovician and Silurian of Tarim Basin, Ordos, Jiangsu areas," *Acta Palaeontologica Sinica*, vol. 39, no. 1, pp. 151–156, 2000.

[37] H. Jacob, "Classification, structure, genesis and practical importance of natural solid oil bitumen ("migrabitumen")," *International Journal of Coal Geology*, vol. 11, no. 1, pp. 65–79, 1989.

[38] H. K. Nie, Z. J. Jin, C. X. Sun, Z. L. He, G. X. Liu, and Q. Y. Liu, "Organic matter types of the Wufeng and Longmaxi Formations in the Sichuan Basin, South China: implications for the formation of organic matter pores," *Energy & Fuels*, vol. 33, no. 9, pp. 8076–8100, 2019.

[39] X. Tang, Z. Jiang, S. Jiang, and Z. Li, "Heterogeneous nanoporosity of the Silurian Longmaxi Formation shale gas reservoir in the Sichuan Basin using the QEMSCAN, FIB-SEM, and nano-CT methods," *Marine and Petroleum Geology*, vol. 78, pp. 99–109, 2016.

[40] R. G. Loucks, R. M. Reed, S. C. Ruppel, and U. Hammes, "Spectrum of pore types and networks in mudrocks and a descriptive classification for matrix-related mudrock pores," *AAPG Bulletin*, vol. 96, no. 6, pp. 1071–1098, 2012.

[41] C. A. Rios and O. M. Castellanos, "Microstructural characterization of pore types in unconventional gas reservoirs utilizing FEG-SEM: an example from the Galembo member of the cretaceous La Luna Formation, Middle Magdalena Valley Basin (Colombia)," *Revista de la Academia Colombiana de Ciencias Exactas, Fisicas y Naturales*, vol. 40, no. 154, pp. 161–175, 2016.

[42] R. G. Loucks and R. M. Reed, "Scanning-electron-microscope petrographic evidence for distinguishing organic-matter pores associated with depositional organic matter versus migrated organic matter in mudrock," *GCAGS Journal*, vol. 3, pp. 51–60, 2014.

[43] Y. Yang and A. C. Aplin, "A permeability-porosity relationship for mudstones," *Marine and Petroleum Geology*, vol. 27, no. 8, pp. 1692–1697, 2010.

[44] R. Sassen, "Geochemical and carbon isotopic studies of crude oil destruction, bitumen precipitation, and sulfate reduction in the deep Smackover Formation," *Organic Geochemistry*, vol. 12, no. 4, pp. 351–361, 1988.